Influence of temperature for the azide displacement in benzodiazepine derivatives: Experimental and DFT study of competing S_N1, S_N2 and double S_N2 reaction pathways

Tereza Cristina Santos Evangelista [a], Maicon Delarmelina [b,c], Dinesh Addla [a], Rafael A. Allão [d], Carlos Roland Kaiser [a], José Walkimar de M. Carneiro [b], Floriano Paes Silva-Jr [e], Sabrina Baptista Ferreira [a,⇑]

[a] LaSOPB – Laboratório de Síntese Orgânica e Prospecção Biológica, Instituto de Química, Universidade Federal do Rio de Janeiro, Rio de Janeiro, RJ 21941-909, Brazil
[b] Instituto de Qu´mica, Universidade Federal Fluminense, Niterói, Rio de Janeiro 24020-141, Brazil
[c] School of Chemistry, Cardiff University, Main Building, Park Place, Cardiff CF10 3AT, United Kingdom
[d] Instituto de Química, Universidade Federal do Rio de Janeiro, Rio de Janeiro, RJ 21941-909, Brazil
[e] LaBECFar – Laboratório de Bioquímica Experimental e Computacional de Fármacos, Instituto Oswaldo Cruz, Fundação Oswaldo Cruz, Rio de Janeiro, RJ 21.040-360, Brazil

article info

Keywords:
Azide
Pyrrolobenzodiazepines
Nucleophilic substitution reactions
Diastereoisomers
Temperature
DFT

abstract

Molecules carrying the azido functionality are widely used as intermediates in medicinal chemistry. Pyrrolobenzodiazepines are molecules with a broad range of interesting pharmacological properties. Due to the wide importance of azido-PBD as a key intermediate in many synthetic pathways, in this work we have investigated the effect of a variety of experimental parameters on the mechanism of nucleophilic substitution reaction for introducing an azide group into the PBD scaffold. This study was carried out by combined experimental and DFT approaches, showing that S_N2 and double S_N2 pathways are possible and highly dependent on the reaction temperature.

Introduction

Pyrrolo[2,1–c][1,4]benzodiazepines (PBD) (1) are a class of nat-urally occurring molecules that can be isolated from Streptomyces bacteria and that exhibit a broad spectrum of biological activities, featuring its antitumor properties as DNA minor groove binding agents. The first PBD molecule isolated was anthramycin (2) [1]. After that, a number of PBD molecules have been isolated from nat-ural sources and efforts have been applied to synthesize new PBD derivatives that also presents pharmacological and biological prop-erties, including anticancer, binding to $GABA_A$ receptor and forma-tion of antibody-drug conjugates (ADCs) [2–6].

PBD molecules consist of a tricyclic structure, including an aro-matic A-ring, a diazepine B-ring and a pyrrolidine C-ring (3), differ-ing from one another specially by substitutions on the A and C rings, and by the degree of unsaturation of the pyrrolidine ring (Fig. 1). All naturally occurring PBD have S configuration at C-11a, which provides a three-dimensional conformation that allows the molecules to fit perfectly in the minor groove of DNA [7].

Concerning the structure activity relationships regarding PBD derivatives as anticancer agents, studies have shown that modifi-cations at the substituents of the C-2 position can significantly alter the DNA-binding ability and the cytotoxicity of the molecules. For example, investigations involving anthramycin showed that the removal of its C-2 side chain led to a strong decline of its DNA binding capacity [8,9]. This effect is due to the location along the minor groove of the extended side chains at C-2. Once accom-modated along the minor groove, the groups of the side chain can interact with the minor groove floor through hydrogen bonds and Van der Waals interactions [1]. Those interactions stabilize the adduct and enhance the DNA binding affinity leading to higher cytotoxic potency. The comprehension of these interactions has helped researchers to design novel PBD analogues including mono-mers and dimers with modifications at the C-2 position, with enhanced DNA binding ability and cytotoxicity (Fig. 1) [2,3].

Therefore, we hypothesized that the addition of a second phar-macophore nucleus as a substituent to the C-2 position in the PBD scaffold, would entail increased DNA binding affinity and therefore

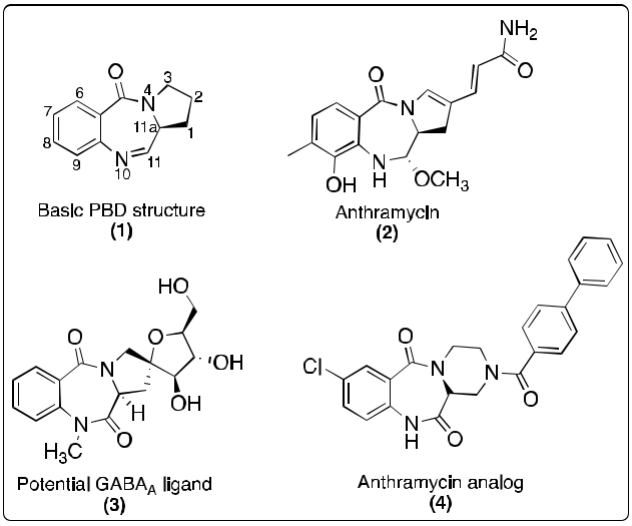

Fig. 1. The pyrrolobenzodiazepine (PBD) scaffold and the structure of pharmaco-logically active PBDs.

pharmacological activity. Triazoles [10], tetrazoles [11], amides [12,13] and its derivatives have shown anticancer activity when linked with another pharmacophore function. These hybrid mole-cules, containing two or more pharmacophore units, can potential-ize the anticancer effect of the PBD core, reduce side effects and overcome other drawbacks associated with PBD derivatives.

Results and discussion

To obtain the triazole and tetrazole heterocycles mentioned above, a suitable key intermediate is the azido group. The azido functionality has been successfully applied in carbohydrate chem-istry [14], synthesis of heterocycles and peptide chemistry [15]. The azido group can be obtained via different reactions, such as substitution or addition via the insertion of the N_3 group, diazoti-zation, diazo transfer, cleavage of triazines and azide rearrange-ment. Among those, the most common method applied for the synthesis of alkyl azides is the classic nucleophilic substitution reaction [16].

In the present work, the azido-PDB derivative was synthesized according to Scheme 1, starting with a condensation reaction between isatoic anhydride and trans-hydroxy-L-proline, followed by the conversion of the hydroxyl functionality into a better leav-ing group. After that, the desired S_N2 reaction with NaN_3 would

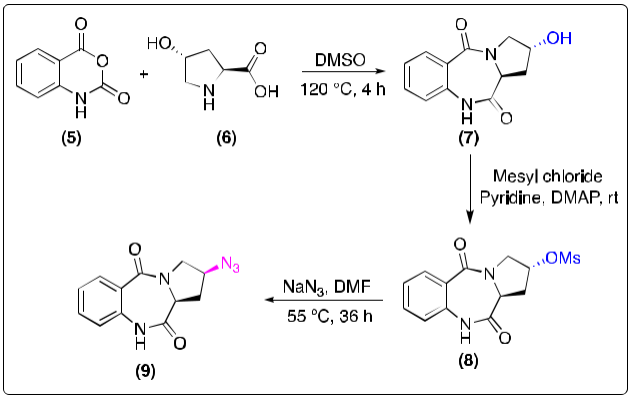

Scheme 1. Synthesis of the azido-PBD from isatoic anhydride and trans-hydroxy-L-proline.

afford the azido-PDB derivative with inversion of configuration at the nucleophilic center.

As presented in Scheme 1, in the first attempt to obtain the azido-PBD derivative, we followed the procedure published by Schultz and collaborators [17] where the reaction was carried out at 55 LC in DMF for 36 h. The product obtained was recrystallized from acetone, affording colorless crystals. The azide displacement went exclusively with inversion of configuration at C-2 leading to one diastereomer as confirmed by NMR elucidation and crystal structure. In order to optimize the reaction, we decided to apply different conditions to the azide displacement, as described by Rault and collaborators [18] that performed the reaction at 100 LC in DMF for 5 h. However, it was not observed a 100% inver-sion of configuration at C-2 under these conditions, leading to a mixture of the two possible azido-PBD diastereomers. Such a result could imply that a change in mechanism is occurring at different temperatures.

In the interest of understanding this phenomenon, different reaction conditions were investigated, including the effect of sol-vents, leaving groups, temperature and reaction times, as pre-sented in Table 1. The reactions were performed using the same ratio between the reactants (1 equiv.) and NaN_3 (5 equiv.) accom-panied by TLC (eluent: ethyl acetate) until all the reactant was con-sumed. The results obtained for the different conditions are presented in Table 1, including the yield and the diastereomeric ratios obtained in the cases where the reactions led to the mixture. The ratio was assigned by ^{1}H NMR analysis, as shown in Fig. 2.

Concerning the solvent choices, the reactions were carried out in DMF and formamide. DMF is a polar aprotic solvent, which can improve the efficiency of the nucleophile in an S_N2-type reac-tion while formamide, besides being a polar solvent, also show the ability to make hydrogen bonds, which is not usually ideal in an S_N2-type reaction. However, it was not observed significant changes concerning the diastereomeric ratio obtained for the dif-ferent reactions, indicating that the solvent is not important in changing the mechanistic pathway in the case of azido-PBD forma-tion. The only difference we could observe between the two sol-vents is the isolated yield, which is higher when using DMF for all reaction conditions (1–3 and 7–9). The reaction time also do not seem to have an impact on the mechanism of the reaction, although as expected longer reaction times were observed for lower temperatures.

The reaction was performed at different temperatures based on previously reported works [16,17]. As discussed before, when the reaction was carried out at 55 LC, just one product was observed, and it was the one corresponding to a 100% inversion of configura-tion at C-2. The same result was observed when applying different leaving groups and solvents, confirming a substitution by direct displacement (S_N2) mechanism (Entries 3, 6, 9 and 12 in Table 1). However, once the temperature was increased to 100 LC, the for-mation of a mixture of diastereomers started to be observed, where the main diastereomer formed was still 9b. The same results were obtained for all the reactions performed at 100 LC, regardless of which leaving group or solvent was used, with diastereomeric ratios similar to one another (Entries 2, 5, 8 and 11). When the reactions were performed at 120 LC, the mixture of diastereomers was observed for all the entries. However, the diastereomeric ratio of the products changed

drastically, leading to the isomer 9a being the major one for en-tries 1, 7 and 10, except for entry 4, where the ratio is close to 50:50.

X-ray crystallography was employed to unequivocally charac-terize stereochemistry and conformation of one of the obtained azido-PBD diastereomers. A single crystal of compound 9b was obtained by slow evaporation of acetone from the solution of pure diastereomer. 9b crystallizes in the P_{21} space group containing one

Table 1
Evaluation of different reaction conditions for the azide displacement reaction.

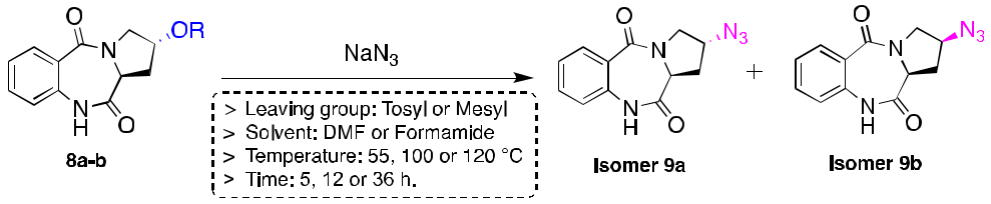

Entry	LG[a]	Temperature	RT[b]	Solvent	^{1}H NMR ratio Isomer 9a: 9b	Yield (%)
1	Tosyl	120 LC	12 h	DMF	Mixture (59:41)	94
2	Tosyl	100 LC	5 h	DMF	Mixture (9:91)	85
3	Tosyl	55 LC	36 h	DMF	(0:100)	85
4	Tosyl	120 LC	12 h	Formamide	Mixture (49:51)	29
5	Tosyl	100 LC	5 h	Formamide	Mixture (15:85)	45
6	Tosyl	55 LC	36 h	Formamide	(0:100)	55
7	Mesyl	120 LC	12 h	DMF	Mixture (63:37)	82
8	Mesyl	100 LC	5 h	DMF	Mixture (36:64)	62
9	Mesyl	55 LC	36 h	DMF	(0:100)	47
10	Mesyl	120 LC	12 h	Formamide	Mixture (65:35)	50
11	Mesyl	100 LC	5 h	Formamide	Mixture (9:91)	46
12	Mesyl	55 LC	36 h	Formamide	1 diastereoisomer	50

[a] Leaving Group.
[b] Reaction time.

independent molecule per unit cell. The asymmetric unit is shown in Fig. 3, and the stereochemistry of C2 confirms that the reaction occurred through S_N2 mechanism. The crystal packing is stabilized by intermolecular hydrogen bonds between oxygen atom O1 and amine group (N2-H7). Each molecule shows intermolecular inter-actions with two other adjacent molecules generating a supramolecular chain along the crystallographic direction b (see Fig. S1 for details).

At the final stage of this investigation, DFT calculations have been applied to provide deeper insight into the effect of tempera-ture over the alternative reaction mechanisms for OMs displace-ment by azide in the investigated benzodiazepine derivatives. Using 8b as substrate for this investigation, the energy profile of three competing reaction channels were computed, S_N1, S_N2 and ''double" S_N2, as shown in Fig. 4. As observed during the experi-mental investigations, the S_N2 pathway (Fig. 4) presented the low-est free energy barrier from 8b (27.2 kcal mol ^{1}), which clearly justify the exclusive formation of product 9b at low reaction tem-peratures. However, with increasing temperature, a mixture of products was observed which raised the hypothesis of a possible change in the observed mechanisms, either via a S_N1 mechanism or via the so-called ''double" S_N2 as proposed by Szabó and Czakó [18,19].

Firstly, we investigated the energy cost to form a carbocation species in the reaction mixture by elimination of the substituent group at C-2 (either OMs or N_3). As described in previous works, computing the energy barriers for formation of such intermediate is, in general, a good approximation to estimate the rate constant

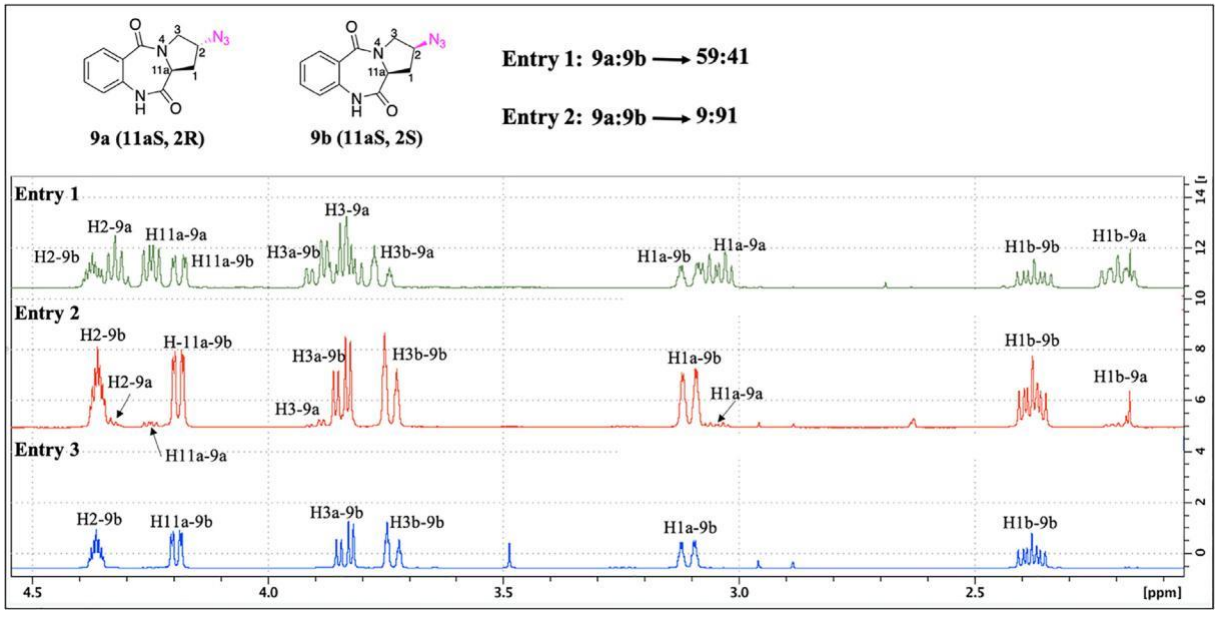

Fig. 2. ^{1}H NMR spectra from aliphatic region used for the determination of the diastereomeric ratio. ($CDCl_3$, 400.13 MHz).

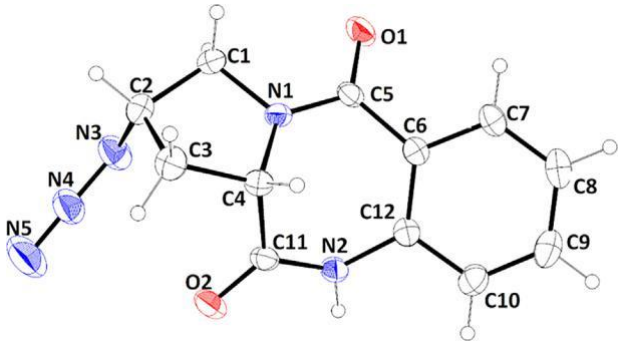

Fig. 3. ORTEP view of the asymmetric unit of 9b with thermal ellipsoids drawn at 30% of probability.

for conventional S_N1 reactions [20]. As it can be seen in Fig. 4, such carbocation would be a highly energetic intermediate, presenting relative free energy higher than 45 kcal mol ^{1} in comparison to the isolated reactants. The possible stabilization of 10 by interac-tions with nucleophile and leaving group was also tested by the construction of a [OMs 10 N_3] complex, however the resulting decrease in energy was smaller than 2 kcal mol ^{1} when the anions were kept 3.5 Å away from the carbocationic center.

On the other hand, the alternative ‘‘double” S_N2 process pre-sents much lower free energy barrier than that to form the above-mentioned carbocation intermediate. Starting from intermediate 9b, which has relative free energy around 21.0 kcal mol ^{1} com-pared to 8b, the activation Gibbs free energy to form the product with a second inversion via a second S_N2 reaction is 37.6 kcal mol ^{1}. Although this is a relatively high energy, requiring heat to be sur-mounted, it is lower than the activation Gibbs free energy for the S_N1 process. As a result, the most favorable process identified here for OMs substitution in 8b is an initial S_N2 reaction, with a Gibbs free energy barrier of 27.2 kcal mol ^{1}, followed by a ‘‘double” S_N2 step presenting a free energy barrier of 37.6 kcal mol ^{1}. These results are consistent with the experimental observation of enan-tioselective formation of 9a and 9b at distinct temperatures. For-mation of 9b occurs with the lowest energy barrier. As this is a stable intermediate, its lifetime is enough to dissipate energy. At low temperature this is the main product formed. Increasing the temperature 9b can be converted into 9a by reaction with excess N_3 in the reaction mixture. Furthermore, the slightly higher stabil-ity of 9a regarding 9b is also consistent with the observation of increased amount of 9a when longer reaction time is used. This observation was investigated experimentally by treating diastere-omerically pure 9b with sodium azide in DMF at 120 LC overnight. This resulted in 63:37 9a:9b ratio, confirming the preference for a ‘‘double” S_N2 pathway at higher temperatures.

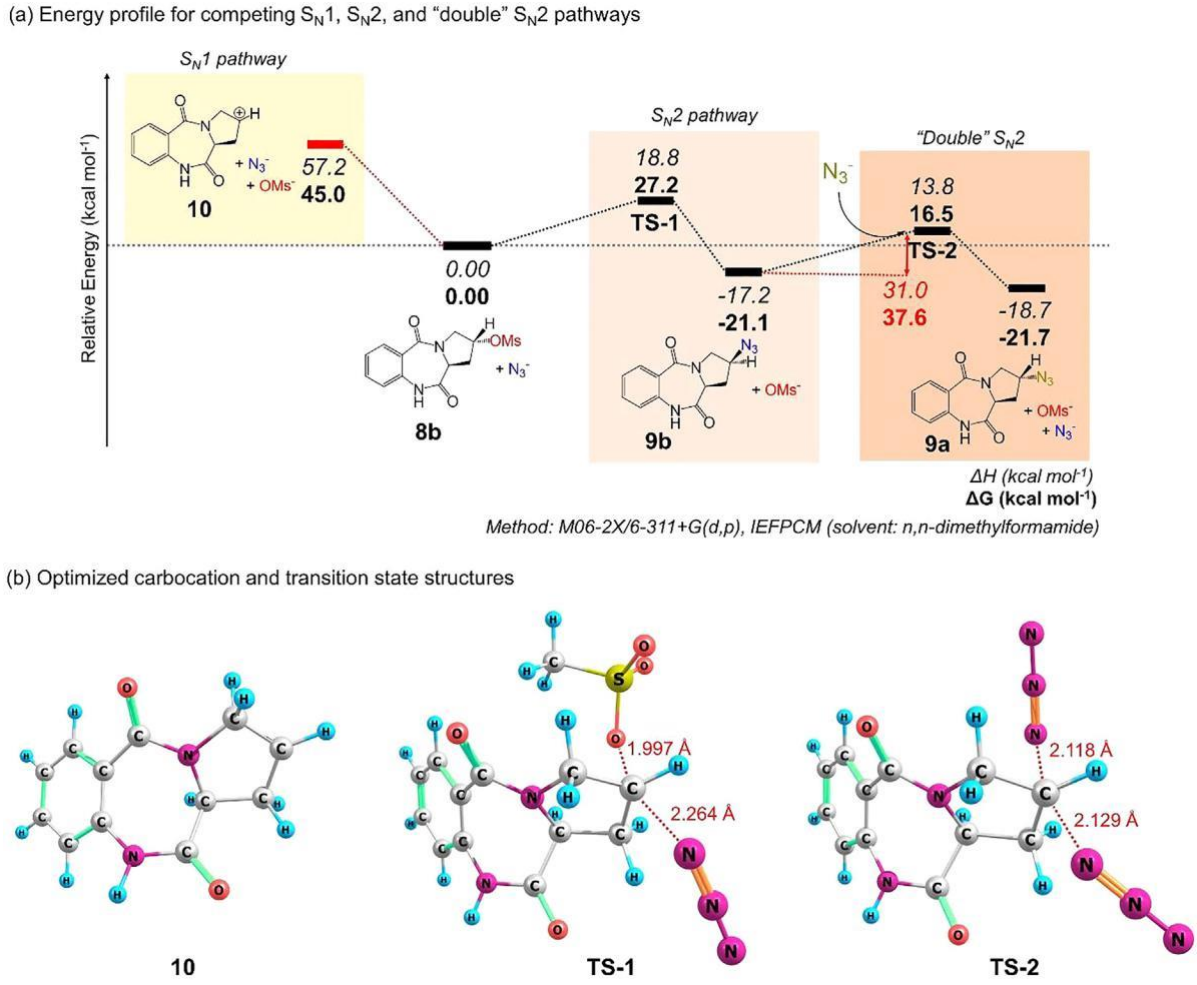

Fig. 4. Computed energy profile for alternative S_N1, S_N2, and ‘‘double” S_N2 reaction pathways for OMs displacement by azide in 8b.

Conclusions

This study showed that small changes in temperature led to retention of configuration in the azide displacement of PBD deriva-tives. This is in contrast to previously reported literature, which describes 100% inversion of configuration at the substitution cen-ter. 1D and 2D-NMR techniques were used to identify products and follow the changes in the reaction over time. Furthermore, X-ray crystallography was employed to unequivocally characterize stereochemistry and conformation of one of the obtained azido-PBD diastereomers. While products with inversion of configuration are the commonly expected outcome for this reaction, we have shown that small changes in the reaction temperature can lead to the diastereomer with retention of configuration. Results of DFT calculations have provided a theoretical insight into the effect of the temperature over the reaction mechanism, showing that a ‘‘double” S_N2 mechanism takes place at higher temperatures, which was confirmed experimentally. Our results can be useful when evaluating the pharmacological profile of molecules pre-pared from key azido-PBD intermediates, where molecules with high enantiomeric purity are required. In addition, the ability to obtain both diastereomers is also an advantage, once it allows for evaluating their pharmacological properties, which can vary considerably.

Declaration of Competing Interest

The authors declare that they have no known competing finan-cial interests or personal relationships that could have appeared to influence the work reported in this paper.

Acknowledgements

The authors acknowledge LDRx-UFF for using its crystallo-graphic facilities. The authors would like to acknowledge CNPq (grants no. 309095/2018-2 and 306836/2017-3), FAPERJ (grant no. E-26/202.743/2019). T.C.S.E. would like to acknowledge Coor-denação de Aperfeiçoamento de Pessoal de Nível Superior – Brasil (CAPES) for a Ph.D. fellowship.

Appendix A. Supplementary data

Supplementary data (detailed experimental procedures, charac-terization data (^{1}H, ^{13}C NMR and HRMS), copies of spectra and fur-ther information concerning DFT studies and X-ray are provided. CCDC 2041317 contains the supplementary crystallographic data as CIF file for this paper. This data can be obtained free of charge from The Cambridge Crystallographic Data Centre via www.ccdc.-cam.ac.uk/structures) to this article can be found online at https://doi.org/10.1016/j.tetlet.2021.152937.

References

[1] J. Mantaj, P.J.M. Jackson, K.M. Rahman, D.E. Thurston, Angew. Chem. Int. Ed. 56 (2017) 462–488.
[2] M.S.K. Sutherland, R.B. Walter, S.C. Jeffrey, P.J. Burke, C. Yu, H. Kostner, I. Stone, M.C. Ryan, D. Sussman, R.P. Lyon, W. Zeng, K.H. Harrington, K. Klussman, L. Westendorf, D. Meyer, I.D. Bernstein, P.D. Senter, R.B. Dennis, J.G. Drachman, A. McEarchem, Blood 122 (2013) 1455–1463.
[3] A. Mieczkowski, M. Psurski, M. Baginski, B. Bieszczad, M. Mroczkowska, M. Wilczek, J. Czajkowska, D. Trzybinski, K. Wozniak, J. Wietrzyk, Bioorg. Med. Chem. Lett. 28 (2018) 618–625.
[4] A.C. Araújo, A.P. Rauter, F. Nicotra, C. Airoldi, B. Costa, L. Cipolla, J. Med. Chem. 54 (2011) 1266–1275.
[5] G.C. Kemp, A.C. Tiberghien, N.V. Patel, F. D’Hooge, S.M. Nilapwar, L.R. Adams, S. Corbett, D.G. Williams, J.A. Hartley, P.W. Howard, Bioorg. Med. Chem. Lett. 27 (2017) 1154–1158.
[6] A.C. Tiberghien, J.N. Levy, L.A. Masterson, N.V. Patel, L.R. Adams, S. Cobert, D.G. Williams, J.A. Hartley, P.W. Howard, ACS Med. Chem. Lett. 7 (2016) 983–987.
[7] J.A. Hartley, Expert. Opin. Investig. Drugs 20 (2011) 733–744.
[8] M.L. Kopka, D.S. Goodsell, I. Baikalov, K. Grzeskowiak, D. Cascio, R.E. Dickerson, Biochemistry 33 (1994) 13593–13610.
[9] S.B. Hoewitz, S.C. Chang, A.P. Grollman, A.B. Borkovec, Science 174 (1971) 159–161.
[10] Z. Xu, S.-J. Xhao, Y. Liu, Eur. J. Med. Chem. (2019) 111700.
[11] L. Lauko, P.H.J. Kouwer, A.E. Rowan, Anti-Cancer Agents Med. Chem. 17 (2017) 1856–1868.
[12] Y. Lu, Z. Wang, C.-M. Lib, J. Chen, J.T. Dalton, W. Li, D.D. Miller, Bioorg. Med. Chem. 18 (2010) 477–495.
[13] T. Sreelatha, S. Kandhasamy, R. Dinesh, S. Shruthy, S. Shweta, D. Mukesh, D. Karunagaran, R. Balaji, N. Mathivanan, Bioorg. Med. Chem. Lett. 24 (2014) 3647–3651.
[14] S.B. Ferreira, A.C.R. Sodero, M.F.C. Cardoso, E.S. Lima, C.R. Kaiser, F.P. Silva-Jr, V. F. Ferreira, J. Med. Chem. 53 (2010) 2364–2375.
[15] I.F. Silva, P.R.C. Martins, E.G. Silva, S.B. Ferreira, V.F. Ferreira, K.R.C. Costa, M.C. Vasconcellos, E.S. Lima, F.C. Da Silva, Med. Chem. 9 (2013) 1085–1090.
[16] Y. Bi, P.G. Schultz, Bioorg. Med. Chem. Lett. 6 (1996) 2299–2300.
[17] A.C. Gillard, M. Alkhader, S. Rault, Heterocycl. Commun. 2 (1996) 409–414.
[18] I. Szabo, G. Czako, Nature Commun. 6 (2015) 5972.
[19] J. Xie, W.L. Hase, Science 352 (2016) 32–33.
[20] N. Streidl, B. Denegri, O. Kronja, H.A. Mayr, Acc. Chem. Res. 43 (2010) 1537– 1549.